J|A|C|S
ARTICLES
Published on Web 04/06/2006

Two-Dimensional Self-Assembly of 1-Pyrylphosphonic Acid: Transfer of Stacks on Structured Surface

Hin-Lap Yip,[†] Hong Ma,[†] Alex K.-Y. Jen,*[,†,‡] Jianchun Dong,[§] and Babak A. Parviz[§]

Contribution from the Department of Materials Science and Engineering, Department of Chemistry, and Department of Electrical Engineering, University of Washington, Seattle, Washington 98195

Received October 3, 2005; E-mail: ajen@u.washington.edu

Abstract: Strong hydrogen bonding and $\pi-\pi$ stacking between 1-pyrylphosphonic acid (PYPA) molecules were exploited to create self-assembled two-dimensional supramolecular structures. Polycrystalline films of these laminate crystalline PYPA bilayers were easily deposited onto the solid supports through a simple spin-coating technique. Atomic force microscopy (AFM), scanning tunneling microscopy (STM), X-ray diffraction (XRD), Fourier transform infrared spectroscopy (FTIR), UV−vis absorption, and fluorescence spectroscopy reveal that processing parameters, such as solvent, concentration, and surface of the substrate, are critical factors in determining the final morphology of the stacked film. Robust laminate structures could be obtained only when short alkyl chain protic solvents (methanol or ethanol) and a nonhydrophobic substrate surface were used. Polycrystalline films were formed through the nucleation and growth of PYPA molecules into laminate structures at the air/solvent interface before they land on the substrate during the spin-coating process. These films possess good mechanical properties and were easily transferred onto a SiO_2/Si substrate that was patterned with Au electrodes without breaking their crystalline structures. The successful transfer of the laminate crystals allows us to probe their electrical properties through a field effect transistor device. A gating effect on the charge transport of the stacked films indicates that PYPA laminate crystal possesses p-typed semiconductor characteristics.

Introduction

Ordered organic solid-state π-conjugated materials possess very attractive electrical and optical properties that can be used for potential applications in field-effect transistors (FETs)[1] and photovoltaic cells (PVs).[2] To improve their properties, the approach of employing noncovalent interactions, such as Coulombic interactions, van der Waals forces, hydrophobic interactions, $\pi-\pi$ stacking, and hydrogen bonding, to create supramolecular self-assembly has been proved as an effective method for controlling the organization of organic semiconductors into desired ordered structures. Through molecular design for functional self-assembly, an impressive array of supramolecular architectures including helices,[3] tubes,[4] grids,[5] boxes,[6] and large cyclic assemblies[7] has been demonstrated. In most of the cases, the self-assembled structures are formed in the solution. To utilize these assemblies as active materials in solid-state optoelectronic devices, they have to be deposited onto solid supports while maintaining their ordered structures. However, it remains a significant challenge to achieve precise control of the nanostructures and preserve their integrity on the surface.[8] To achieve better device characteristics, it is critical to understand the mechanisms and processing parameters that could

[†] Department of Materials Science and Engineering.
[‡] Department of Chemistry.
[§] Department of Electrical Engineering.

(1) (a) Sirringhaus, H.; Brown, P. J.; Friend, R. H.; Nielsen, M. M.; Bechgaard, K.; Langeveld-Voss, B. M. W.; Spiering, A. J. H.; Janssen, R. A. J.; Meijer, E. W.; Herwig, P.; de Leeuw, D. M. *Nature* **1998**, *401*, 685−688. (b) van de Craats, A. M.; Stutzmann, N.; Bunk, O.; Nielsen, M. M.; Watson, M.; Mullen, K.; Chanzy, H. D.; Sirringhaus, H.; Friend, R. H. *Adv. Mater.* **2003**, *15*, 495−499. (c) Facchetti, A.; Mushrush, M.; Yoon, M. H.; Hutchison, G. R.; Ratner, M. A.; Marks, T. J. *J. Am. Chem. Soc.* **2004**, *126*, 13859−13874. (d) Wu, Y.; Li, Y.; Gardner, S.; Ong, B. S. *J. Am. Chem. Soc.* **2004**, *127*, 614−618.

(2) (a) Schmidt-Mende, L.; Fechtenkotter, A.; Mullen, K.; Moons, E.; Friend, R. H.; MacKenzie, J. D. *Science* **2001**, *293*, 1119−1122. (b) Yang, X. N.; van Duren, J. K. J.; Rispens, M. T.; Hummelen, J. C.; Janssen, R. A. J.; Michels, M. A. J.; Loos, J. *Adv. Mater.* **2004**, *16*, 802−806.

(3) (a) Koert, U.; Harding, M. M.; Lehn, J. M. *Nature* **1990**, *346*, 339−342. (b) Engelkamp, H.; Middelbeek, S.; Nolte, R. J. M. *Science* **1999**, *284*, 785−788. (c) Hirschberg, J. H. K. K.; Brunsveld, L.; Ramzi, A.; Vekemans, J. A. J. M.; Sijbesma, R. P.; Meijer, E. W. *Nature* **2000**, *407*, 167−170. (d) Percec, V.; Glodde, M.; Bera, T. K.; Miura, Y.; Shiyanovskaya, I.; Singer, K. D.; Balagurusamy, V. S. K.; Heiney, P. A.; Schnell, I.; Rapp, A.; Spiess, H.-W.; Hudson, S. D.; Duan, H. *Nature* **2002**, *419*, 384−387.

(4) (a) Ghadiri, M. R.; Granja, J. R.; Milligan, R. A.; Mcree, D. E.; Khazanovich, N. *Nature* **1993**, *366*, 324−327. (b) Yan, D. Y.; Zhou, Y. F.; Hou, J. *Science* **2004**, *303*, 65−67. (c) Hill, J. P.; Jin, W. S.; Kosaka, A.; Fukushima, T.; Ichihara, H.; Shimomura, T.; Ito, K.; Hashizume, T.; Ishii, N.; Aida, T. *Science* **2004**, *304*, 1481−1483. (d) Shimizu, T.; Masuda, M.; Minamikawa, H. *Chem. Rev.* **2005**, *105*, 1401−1444.

(5) (a) Baxter, R. N. W.; Lehn, J. M.; Fischer, J.; Youinou, M. T. *Angew. Chem., Int. Ed. Engl.* **1994**, *33*, 2284−2287. (b) Weissbuch, I.; Baxter, P. N. W.; Cohen, S.; Cohen, H.; Kjaer, K.; Howes, P. B.; Als-Nielsen, J.; Hanan, G. S.; Schubert, U. S.; Lehn, J. M.; Leiserowitz, L.; Lahav, M. *J. Am. Chem.* Soc. **1998**, *120*, 4850−4860. (c) Ruben, M.; Rojo, J.; Romero-Salguero, F. J.; Uppadine, L. H.; Lehn, J. M. *Angew. Chem., Int. Ed.* **2004**, *43*, 3644−3662.

(6) (a) Stang, P. J.; Zhdankin, V. V. *J. Am. Chem. Soc*. **1993**, *115*, 9808−9809. (b) Tsuda, A.; Nakamura, T.; Sakamoto, S.; Yamaguchi, K.; Osuka, A. *Angew. Chem., Int. Ed.* **2002**, *41*, 2817−2821. (c) Lang, J. P.; Xu, Q. F.; Chen, Z. N.; Abrahams, B. F. *J. Am. Chem. Soc.* **2003**, *125*, 12682−12683.

(7) (a) Harada, A.; Li, J.; Kamachi, M. *Nature* **1992**, *356*, 325−327. (b) Amabilino, D. B.; et al. *J. Am. Chem. Soc.* **1995**, *117*, 1271−1293. (c) Park, K. M.; Kim, S. Y.; Heo, J.; Whang, D.; Sakamoto, S.; Yamaguchi, K.; Kim, K. *J. Am. Chem. Soc*. **2002**, *124*, 2140−2147.

10.1021/ja0563152 CCC: $33.50

be used to manipulate the self-assembled structures and the transferring process.

Among the different supramolecular self-assembled structures based on the π-conjugated system, the one-dimensional assemblies are the most commonly studied, while the two-dimensional self-assembled laminate structures are comparatively unexplored. Typical examples of self-assembled laminate structures are those generated through 2D hydrogen-bonding networks involving the interactions of guanidinium organosulfonates,[9] sulfamide, or trimesic acid.[10] Organophosphonic acids have also frequently been mentioned to form layered organic−inorganic hybrid frameworks through the interactions between metal ions and the phosphate groups.[11−12]

In term of processing methods used to achieve ordered, layered supramolecular structures, the Langmuir−Blodgett (LB) technique is a commonly adapted one for obtaining desirable architectures to study their photophysical properties. For example, pyrene excimer formation in LB assemblies with pyrene covalently linked to an amphiphilic molecule is one of the most extensively studied systems due to its broad applications as molecular probes in microenvironments.[13,14] In some of those LB layered structures, the pyrene moieties are packed in a face-to-face arrangement with long-range ordering,[15] as opposed to the commonly observed edge-to-face herringbone arrangement in unsubstituted pyrene crystal.[16] This kind of packing is closely related to those observed for anthracene and pentacene crystals, which are being actively investigated for coherent charge transport. Although this technique is very useful for generating a variety of desired structures, it is tedious to operate. The relatively slow speed for producing large area coverage on substrates also limits its practical use for devices. Therefore, it would be ideal if a simple method can be developed to produce self-assembled materials with desirable properties for device applications.

Here, we report the preliminary results of using an amphiphilic aromatic phosphonic acid as a new type of self-assembling motif to generate a 2D laminate architecture through a simple spin-coating process. We propose a new self-assembly mechanism in which the PYPA assemblies did not pre-exist in the starting solution but were formed at the air/alcohol interface during the spin-coating process when the solvent evaporated. Polycrystalline films composed of PYPA 2D laminate crystals can be easily deposited onto the solid supports. Three other molecules including diethyl 1-pyrylphosphonate (PYPDEt), *n*-octadecylphosphonic acid (ODPA), and phenylphosphonic acid (PhPA) were chosen to testify the role of $\pi-\pi$ stacking and hydrogen bonding in the self-assembly process and provide direct comparison to the PYPA molecule. Atomic force microscopy (AFM), scanning tunneling microscopy (STM), X-ray diffraction (XRD), and Fourier transform infrared spectroscopy (FTIR) have been used to study the morphology and internal structure of the PYPA laminate crystals. UV−vis absorption and fluorescence spectroscopy have been used to investigate the effects of solvent, concentration, and substrate on the self-assembly process and to elucidate the self-assembly and deposition mechanisms. Finally, these highly ordered stacks were transferred onto Au-patterned SiO_2/Si substrate for measurement of their electrical properties.

Experimental Section

The synthesis of 1-pyrylphosphonic acid started from the lithiation of 1-bromo-pyrene to prepare diethyl 1-pyrylphosphonate. The diethyl 1-pyrylphosphonate was converted first to di(trimethylsilyl) 1-pyrylphosphonate by reacting with bromotrimethylsilane and then hydrolyzed to form the final product (see Supporting Information). Phenylphosphonic acid (PhPA) and *n*-octadecylphophonic acid (ODPA) were purchased from Aldrich and Alfa Aesar, respectively. Digital Instruments Multimode Nanoscope III scanning probe microscope installed with etched silicon tips with a typical resonant frequency of 300−350 kHz and a chemically etched Pt/Ir tip were used to perform AFM and STM studies, respectively. The X-ray diffraction was performed with a 12 kW Rigaku rotating anode X-ray generator with a double crystal diffractometer. Several types of substrates were used as solid supports for PYPA. Silicon wafers and glass substrates were precleaned with oxygen plasma for 3 min to produce a hydrophilic surface. Polycrystalline Au(111)/mica substrates were obtained from Molecular Imaging Inc. and used without any further surface treatment. The HOPG substrates obtained from Alfa Aesar were first cleaved to produce a fresh surface before the deposition of PYPA. The size of all of the substrates is 1 cm $\times$ 1 cm. During the spin-coating process, 30 μL of PYPA solution was dropped onto the substrate and the spin speed and the spin time were 1000 rpm and 80 s, respectively. For photophysical experiments, transmission FTIR (Perkin-Elmer 1720), UV−vis absorption (Perkin-Elmer Lambda 9), and photoluminescence measurements (Oriel Instaspec IV) of PYPA solution and solid films were performed at room temperature.

The SiO_2/Si substrates patterned with inter-digitated Au electrodes were used as a platform to test charge transport of the stacked PYPA film. The electrodes were fabricated by growing a 60 nm thick dry thermal oxide on highly doped n-type 3" silicon wafers with 0.01−0.02 Ω cm resistivity at 1100 °C for 45 min. A 250-nm-thick poly(methyl methacrylate) (PMMA) layer was spin-coated on the SiO_2 surface, and electron beam lithography was then used to selectively expose the PMMA to generate the electrode pattern. The lateral spacing between the electrodes varies between hundreds of nanometers to micrometers, and the total length of the junction formed between the electrode fingers is 1 mm. Following exposure and development, the PMMA was postbaked for 30 min at 95 °C and then 5 nm of chromium and 100 nm of gold were evaporated onto the chip, respectively. The drain and source electrodes were defined by metal liftoff in acetone after sonicating for 10 min and rinsing in 2-propanol. To form a contact to the gate electrode, a Cr/Au layer was evaporated on an opening that was scratched through the silicon dioxide layer to reach the underlying low resistivity silicon substrate. The charge transporting property of

(8) (a) Jonkheijm, P.; Hoeben, F. J. M.; Kleppinger, R.; van Herrikhuqzen, J.; Schenning, A. P. H. J.; Meijer, E. W. *J. Am. Chem. Soc.* **2003**, *125*, 15941−15949. (b) Nguyen, T. Q.; Martel, R.; Avouris, P.; Bushey, M. L.; Brus, L.; Nuckolls, C. *J. Am. Chem. Soc.* **2004**, *126*, 5234−5242. (c) Leclere, P.; Surin, M.; Viville, P.; Lazzaroni, R.; Kilbinger, A. F. M.; Henze, O.; Feast, W. J.; Cavallini, M.; Biscarini, F.; Schenning, A. P. H. J.; Meijer, E. W. *Chem. Mater.* **2004**, *16*, 4452−4466. (d) Hoeben, F. J. M.; Jonkheijm, P.; Meijer, E. W.; Schenning, A. P. H. J. *Chem. Rev.* **2005**, *105*, 1491−1546.
(9) (a) Russell, V. A.; Ward, M. D. *Chem. Mater.* **1996**, *8*, 1654−1666. (b) Russell, V. A.; Evans, C. C.; Li W.; Ward, M. D. *Science* **1997**, *276*, 575−579. Horner, M. J.; Holman, K. T.; Ward, M. D. *Angew. Chem., Int. Ed.* **2001**, *40*, 4045−4048.
(10) Biradha, K.; Dennis, D.; MacKinnon, V. A.; Sharma, C. V. K.; Zaworotko, M. J. *J. Am. Chem. Soc.* **1998**, *120*, 11894−11903.
(11) (a) Katz, H. E.; Scheller, G.; Putvinski, T. M.; Schilling, M. L.; Wilson, W. L.; Chidsey, C. E. D. *Science* **1991**, *254*, 1485−1487. (b) Cao, G.; Hong, H. G.; Mallouk, T. E. *Acc. Chem. Res.* **1992**, *25*, 420−427. (c) Clearfield, A.; Sharma, C. V. K.; Zhang, B. P. *Chem. Mater.* **2001**, *13*, 3099−3112. (d) Vioux, A.; Le Bideau, J.; Mutin, P. H.; Leclercq, D. *Top. Curr. Chem.* **2004**, *232*, 145−174.
(12) (a) Sharma, C. V. K.; Clearfield, A. *J. Am. Chem. Soc.* **2000**, *122*, 4394−4402. (b) Mahmoudkhani, A. H.; Langer, V. *J. Mol. Struct.* **2002**, *609*, 97−108.
(13) Winnik, F. M. *Chem. Rev.* **1993**, *93*, 587−614.
(14) Matsui, J.; Mitsuishi, M.; Miyashita, T. *Macromolecules* **1999**, *32*, 381−386.
(15) Olszak, T. A.; Willig, F.; Durfee, W. S. *Acta Crystallogr.* **1989**, *C45*, 803−805.
(16) Robinson, J. M.; White, J. G. *J. Chem. Soc.* **1947**, 358−368.

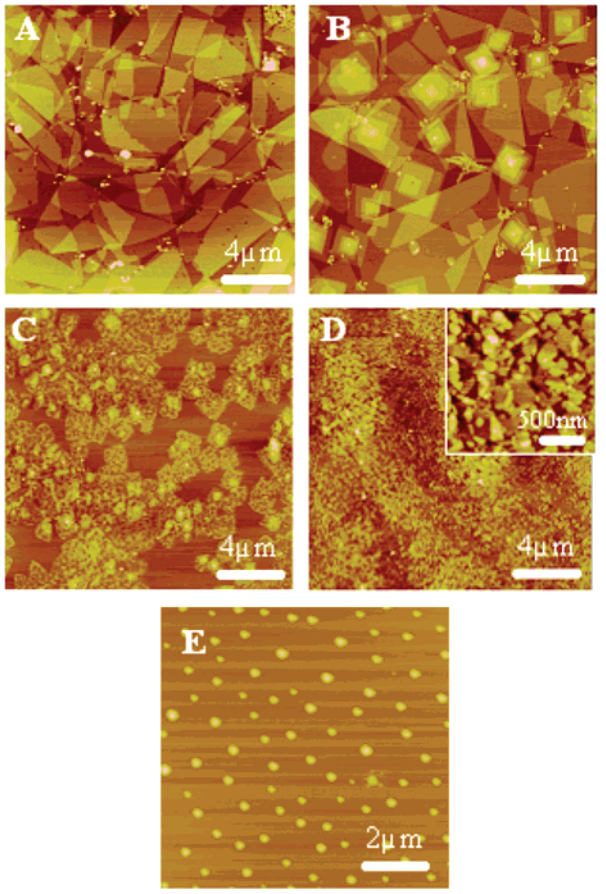

Figure 1. Tapping mode AFM images of PYPA/SiO_2 deposited from a 1 mM solution of (A) methanol, (B) ethanol, (C) 1-propanol, (D) tetrahydrofuran, and (E) *N*,*N* -dimethylformamide. In all cases, 30 μL of solution was deposited on a 1 cm $\times$ 1 cm SiO_2/Si wafer pretreated with oxygen plasma. The spin-coating speed and time were 1000 rpm and 80 s, respectively.

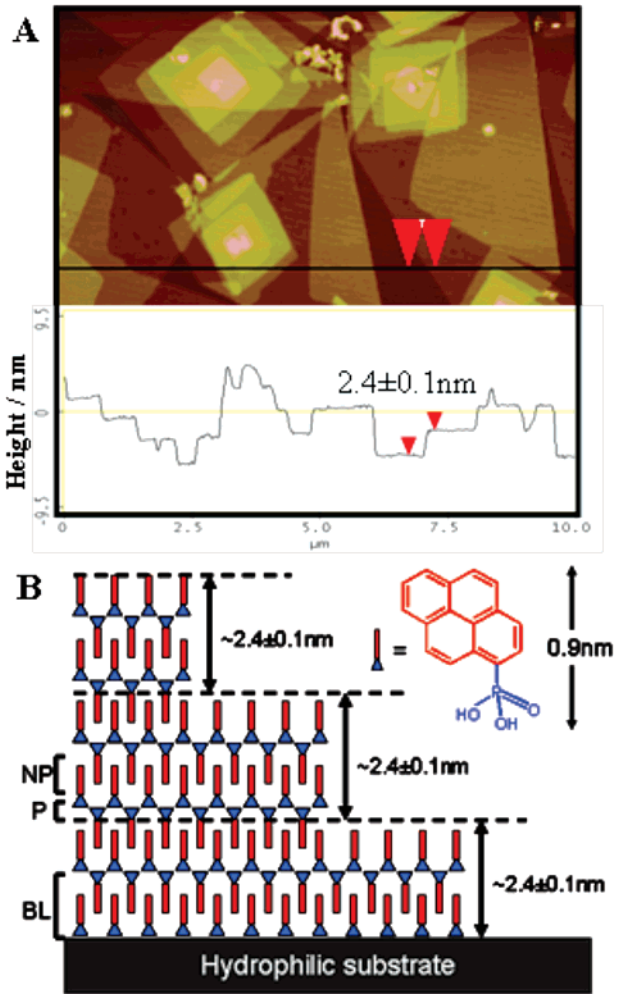

Figure 2. (A) Height profile of PYPA laminate crystals spin-coated on a SiO_2/Si wafer from 1 mM ethanol. (B) Schematic illustration of the proposed PYPA orientation in spin-coated films. The layer adjoining the hydrophilic substrate is the phosphonic acid headgroup, and the one exposed to air is the pyrene endgroup. Inset: Molecular structure of PYPA.

the stacked PYPA films was studied in a cryogenic probe station with a base pressure of 2×10^{-7} Torr.

Results and Discussion

Effects of Solvent on Morphology of the Self-Assembled Structure. A tapping mode AFM was used to study the morphology of the PYPA laminate crystals on solid supports. Figure 1 shows the AFM images of PYPA spin-coated from different solvents on bare SiO_2/Si wafer. When the PYPA was spin-coated from the solutions using short alkyl chain protic solvents such as methanol (Figure 1A) or ethanol (Figure 1B), the laminate structures were formed. The laminate crystals appear to be square-shaped and of micrometer size. They were randomly distributed on the substrate and stacked on each other to form a continuous polycrystalline film. The morphology of the stacked film is very different from the polycrystalline organic thin films deposited by evaporation in a vacuum,[17] in which the growth mechanism is always governed by surface nucleation followed by island growth and each crystalline island never stacks on another crystalline grain. In our case, the PYPA laminate crystals were not nucleated and grown from the surface but formed at the air/alcohol interface prior to landing on the surface. Furthermore, the PYPA laminate crystals contain slide planes perpendicular to the lamellar plane so that when part of a crystal lands onto the other crystal, the overlapped portion of the former crystal can stack on the latter one while the nonoverlapped portion of the former crystal slides down along the edge of the latter one and lands on the substrate.

Figure 2A shows the height profile of the PYPA laminate crystals deposited from ethanol. The AFM image clearly shows that the PYPA crystals form a multilamellar structure with a step-height of 2.4 $\pm$ 0.1 nm in each layer. A schematic illustration of the proposed internal structure of the lamellae is shown in Figure 2B. Each layer is composed of a double interdigitated bilayer with alternating polar regions of 2D phosphonic acids (denoted as P) and nonpolar regions of π-stacked interdigitated pyrene moieties (denoted as NP). Usually, strong H-bonding with bond energies in the range of 15−40 kcal/mol can be formed between the phosphonic acids.[18] The formation of hydrogen bonding between the phosphonic acids in the PYPA polycrystalline film was confirmed by FTIR study (see Supporting Information Figure S1). The layer adjoining the hydrophilic SiO_2 surface is the phosphonic acid headgroup because

(17) (a) Heringdorf, F. J. M. Z.; Reuter, M. C.; Tromp, R. M. *Nature* **2001**, *412*, 517−520. (b) Merlo, J. A.; Newman, C. R.; Gerlach, C. P.; Kelly, T. W.; Muyres, D. V.; Fritz, S. E.; Toney, M. F.; Frisbie, C. D. *J. Am. Chem. Soc.* **2005**, *127*, 3997−4009.

(18) Steiner, T. *Angew. Chem., Int. Ed.* **2002**, *41*, 48−76.

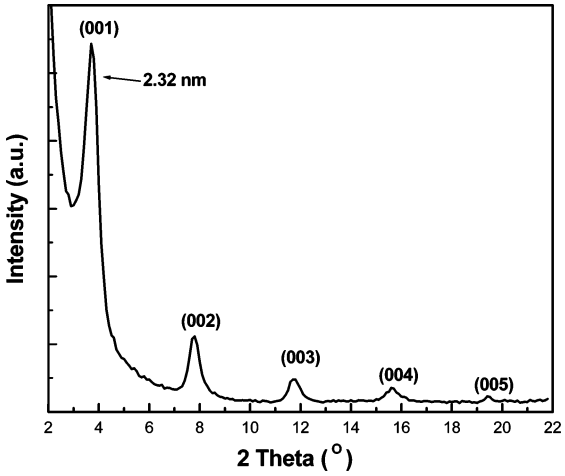

Figure 3. X-ray diffraction pattern of PYPA polycrystalline film on SiO_2/Si substrate.

it can form H-bonding with the hydroxylated surface. The layer that is exposed to air is the hydrophobic pyrene moieties, which is evident by the change of the static contact angle from 0° (the hydroxylated substrate) to 80 ± 3° (the spin-coated film). A similar type of bilayer crystal packing has also been reported before in guanidinium organosulfonate[9] and metal organophosphate[11] systems. The molecular ordering within the interlayer was studied by XRD. The X-ray diffraction pattern of a 20-nm-thick PYPA polycrystalline thin film exhibited the (00*l*) reflections up to fifth order (Figure 3). The primary peak at $2\theta = 3.80°$ corresponds to a *d* spacing of 2.32 nm, which is in good agreement with the step-height of 2.4 ± 0.1 nm of the PYPA crystal obtained from the cross-sectional analysis of the AFM image.

Solvent plays an important role in forming the laminate crystals. Robust laminate crystals could only be formed when PYPA was deposited from short alkyl chain, protic solvents, such as methanol or ethanol. When a similar protic solvent with a slightly longer chain (1-propanol or 1-butanol) was used, imperfect laminate structures were found with defect sites throughout the whole layer (Figure 1C). Figure 1D shows the morphology of PYPA deposited from polar aprotic THF, an uncharacteristic thin film composed of sub-hundred-nanometer grains. When the PYPA was deposited from even more polar, but aprotic DMF, only clusters of PYPA aggregates were formed on the surface (Figure 1E). The effect of solvent on this self-assembled system is quite complicated, and all of the interactions between the vapor−solvent, solvent−molecule, and solvent−substrate are critical for forming the laminate polycrystalline film.

Effect of Concentration on Morphology of the Self-Assembled Structure. The effect of concentration on the self-assembled structure was also studied by depositing PYPA onto a SiO_2/Si wafer from an ethanol solution with the concentration ranging from 0.1 to 2 mM. Figure 4A shows the morphology of PYPA deposited from a 0.1 mM solution. The surface of the substrate is partially covered with flat islands, which are composed of a monolayer of PYPA. The height of the island shown in the inset of Figure 4A is ~0.9 ± 0.1 nm, which is consistent with that of the PYPA molecule (0.9 nm). When the concentration was increased to 0.5 mM, a double bilayer structure with layer heights of 2.4 ± 0.1 nm appears (Figure

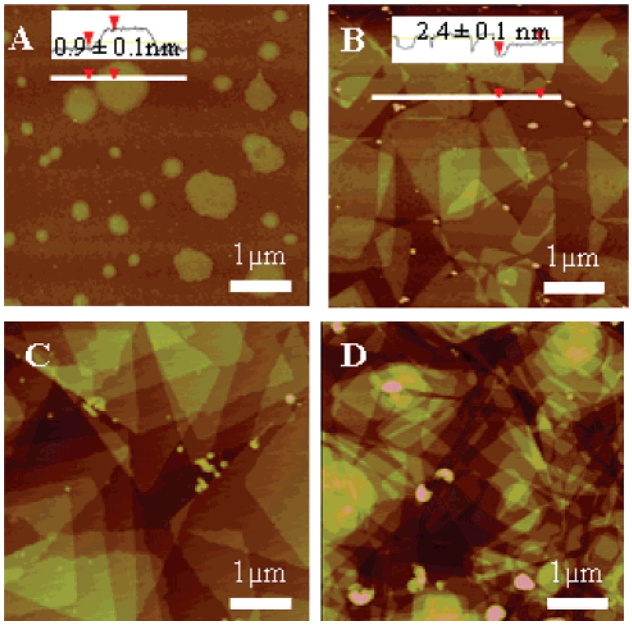

Figure 4. AFM images of PYPA spin-coated from (A) 0.1 mM, (B) 0.5 mM, (C) 1 mM, and (D) 2 mM ethanol on a SiO_2/Si substrate.

4B) and the surface of the substrate was mainly covered by two to three stacked layers. Further increase of the concentration results in the increase in the number of stacked layers. For example, when the concentration was increased to 1 mM, a pyramidal structure composed of four to five stacked layers was found (Figure 4C). A highly stacked film with over 10 stacked layers could be achieved when the concentration was further increased to 2 mM (Figure 4D).

Effect of Substrate on Morphology of the Self-Assembled Structure. The interaction between molecule and substrate is another critical factor that determines whether the stacks formed in solution can be successfully transferred onto the surface without destroying their structures.[6c,8a,b] Four types of substrates with different surface properties, including a hydrophilic SiO_2/Si wafer, a hydrophilic glass, an inert Au(111) film, and a hydrophobic HOPG, were used to investigate the substrate effect. All samples were prepared by spin-coating 30 μL of 1 mM PYPA ethanol solution onto the 1 cm × 1 cm substrates at 1000 rpm. Figure 5 shows the AFM images of the PYPA stacks on different substrates. In the case of SiO_2/Si (Figure 5A), as mentioned earlier, pyramidal structures of stacked layers were formed and the phosphonic acid endgroups located at the bottom of the structure form H-bonding with the hydroxylated surface. Similar stacked layers could also be formed on the hydrophilic glass substrate for the above-mentioned reason. The small fluctuation of height at the surface of the laminate crystals shown in Figure 5B was due to an increase in the surface roughness of the glass substrate. The crystals could also be successfully deposited on the Au(111)/mica surface (indicated by the arrows shown in Figure 5C). Because neither H-bonding with the phosphonic acid nor van der Waals interactions with the pyrene moiety can be formed with the Au surface, it is considered an inert surface to the self-assembled structure. In this case, the laminate crystals just physically deposited on the Au surface when the solvent evaporated; therefore, the crystal structure was retained. The robust crystal formation on Au surface allowed us to study the molecular ordering on the surface

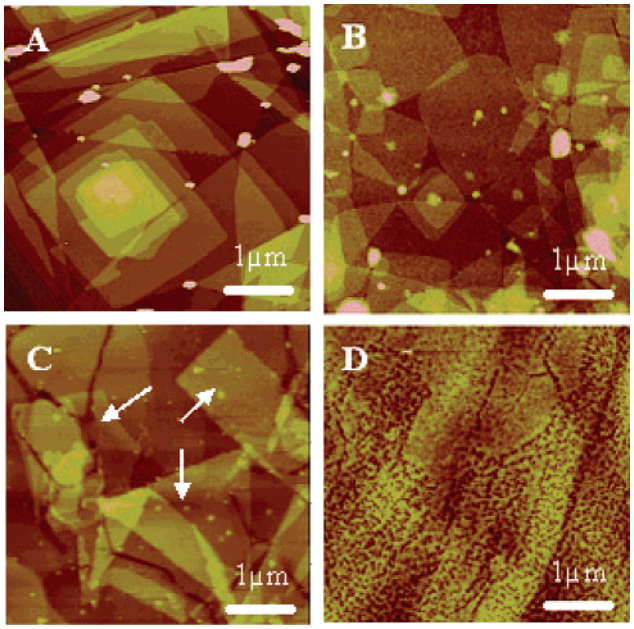

Figure 5. AFM images of PYPA spin-coated from 1 mM ethanol on (A) hydrophilic SiO_2/Si wafer, (B) hydrophilic glass substrate, (C) inert Au-(111)/mica film, and (D) hydrophobic HOPG.

of the crystal through scanning tunneling microscopy (see Supporting Information Figure S2). When the solution was spin-coated on the hydrophobic HOPG, a discontinuous film with no laminate structure was obtained (Figure 5D). We propose that this is due to the incompatibility between the interface of the hydrophilic phosphonic acid 2D sheet of the PYPA crystal and the hydrophobic HOPG surface. This highly energetic interface resulted in the collapse of the crystal structure.[19]

Spectroscopic Studies of PYPA in both Solution and Films. UV−vis absorption and fluorescence spectroscopy were used to study the photophysical and self-assembly characteristics of PYPA in solution and in solid state. Figure 6A shows the absorption spectra of PYPA in different solvents. The absorption spectra of PYPA in all of the solvents consist of sharp and intense bands in the region of 260−380 nm, which is in good agreement with the pyrene absorption peak reported in the literature.[13] As compared to the absorption spectrum in ethanol, a small red shift (2 nm in THF and 3 nm in DMF) was observed. This result indicates that the absorption spectrum is sensitive to the polarity of solvents[20] and the $\pi-\pi^*$ excited state is better stabilized in the polar solvents.

Because aggregation often results in broadened and red-shifted absorption peaks[21] and this phenomenon is often concentration dependent, we have also investigated the steady-state emission spectrum of PYPA in different solutions to extract some useful information from its aggregation behavior (Figure 6B). The characteristic PYPA monomer emission, with the (0,0) band at 392 nm, can be found in all solutions; however, a broad excimer emission centered around 480 nm can only be found in DMF and THF. The presence of excimer emission suggests the formation of aggregates in DMF and THF, while the absence

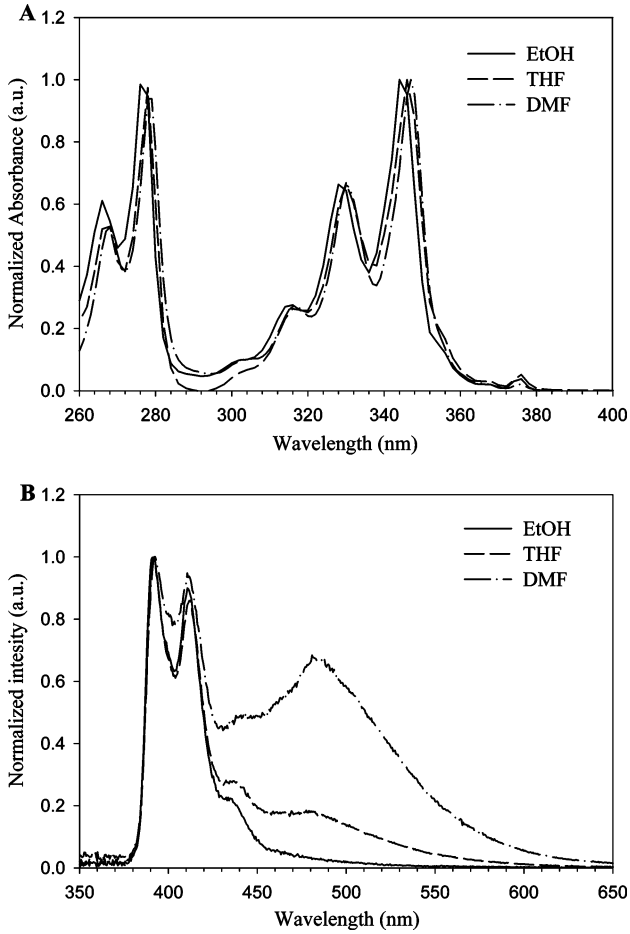

Figure 6. (A) UV−vis absorption spectrum of 1 mM PYPA in different solvents. (B) Fluorescence spectrum of 1 mM PYPA in different solvents excited at 346 nm.

of the excimer peak in ethanol implies that the PYPA molecules are well dispersed in the solution. The morphology of PYPA deposited from the DMF solution in Figure 1E corresponds to the direct transfer of aggregates from the solution onto the substrate. These aggregates appeared as uncharacteristic clusters randomly distributed on the SiO_2/Si substrate. The aggregates in THF can also be transferred onto the substrate to form a continuous thin film (Figure 1D). In the case of ethanol, Because PYPA does not form aggregates in solution, the formation of laminate crystals on the substrate suggests that these supramolecular self-assembled structures are not from the direct transfer of preorganized structures. Therefore, a new mechanism is proposed in the next section to explain the formation of the PYPA laminate stacks during the deposition process.

To study the photophysics of the PYPA crystals in solid state, absorption and fluorescence spectroscopy were performed on the laminate crystals prepared by spin-coating PYPA ethanol solution on a glass substrate. The morphology of the corresponding sample is shown in Figure 5B. Figure 7 shows the absorption and emission spectra of PYPA stacked film on glass. A significant broadening and red shift in the absorption spectrum (~20 nm) was visible in the solid sample. A set of well-resolved vibronic peaks between 300 and 400 nm also suggests that long-range order exists in PYPA aggregates. This is in good agreement with the morphology of PYPA laminate crystal observed under AFM. Further analysis between the relationship

(19) Fontes, G. N.; Neves, B. R. A. *Langmuir* **2005**, *21*, 11113−11118.
(20) Karpovich, D. S.; Blanchard, G. J. *J. Phys. Chem.* **1995**, *99*, 3951−3958.
(21) (a) Kunjappu, J. T.; Somasundaran, P. *Langmuir* **1995**, *11*, 428−432. (b) Dutta, A. K.; Misra, T. N.; Pal, A. J. *Langmuir* **1996**, *12*, 459−465. (c) Matsui, J.; Mitsuishi, M.; Miyashita, T. *J. Phys. Chem. B* **2002**, *106*, 2468−2473.

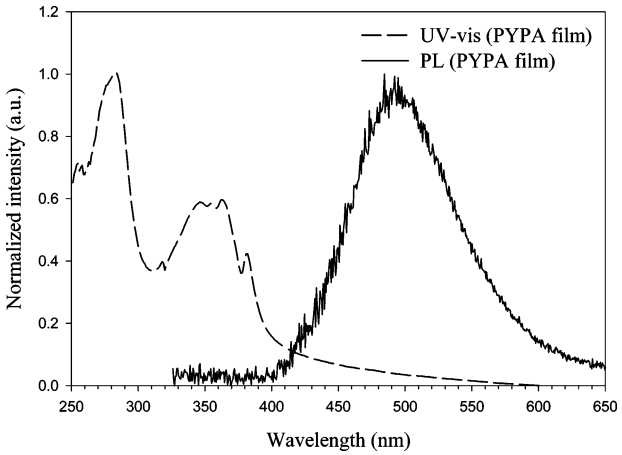

Figure 7. UV−vis absorption and fluorescence spectra of PYPA polycrystalline film deposited on glass substrate from ethanol solution.

of the ratio of different absorption peaks and the orientation of the molecules was discussed in the Supporting Information (Figure 3S). The fluorescence spectrum of PYPA film (excited at 346 nm) also shows a broad and featureless single excimer emission peak (λ_{max} at 495 nm) that is often observed in the crystalline pyrene system.[19]

Proposed Mechanism for the Self-Assembly of PYPA Laminate Crystals from Its EtOH Solution. As we discussed in the previous section, the formation of PYPA crystals on solid supports is not through the direct transfer of its preorganized structures from the ethanol solution to the surface. We propose a new self-assembly mechanism in which the PYPA laminate crystals were formed at the air/ethanol interface during the spin-coating process before coming to rest on the substrate surface when the solvent evaporated. The proposed mechanism is illustrated in Scheme 1. We also observed a distinct emission color change from violet-blue to green during spin-coating due to the change of PYPA from its monomeric form in ethanol to the aggregated form in the laminate crystals. Therefore, it would be very informative if we could monitor the change of emission color during the spin-coating process (under UV light excitation) to study the kinetics of the crystal formation.

The spin-coating process started with the deposition of an excess amount of PYPA ethanol solution onto SiO_2/Si substrate. At this stage, the solvent provides a strong screening effect that can effectively prevent the self-assembling interaction between the PYPA molecules. This results in a relatively strong blue emission, which originates from the PYPA monomer. At the next stage, when the spinner was turned on, most of the solution was spun away from the substrate, resulting in substantially fewer PYPA molecules in the solution. The emission color becomes pale blue as the number of the chromophores decreases. During the spinning process, the solvent starts to evaporate but the number of PYPA molecules in the solution remains the same. In other words, the concentration of the solution on the substrate increases with the spin-coating time. After spinning for ~40 s, a strong green emission is visible on the surface and this red-shifted emission corresponds to the emission from the PYPA excimer, which implies the starting point of the laminate crystal formation. We propose that the self-assembly process starts at a critical concentration in which the molecules are close enough to interact with each other and the screening effect of the solvent is overpowered. Moreover, the nucleation of the

Scheme 1. A Schematic Illustration of the Proposed Self-Assembly Mechanism during the Spin-Coating of PYPA from Ethanol Solution

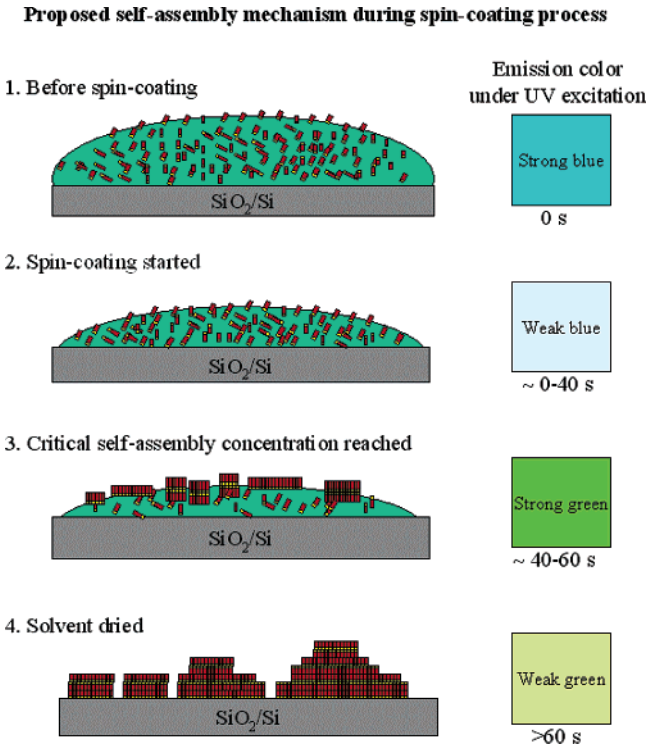

laminate crystal starts at the air/ethanol interface in which the pyrene moieties form $\pi-\pi$ stacking to each other and this hydrophobic pyrene layer points toward the air. At the alcohol side, the hydrophilic phosphonic acid groups form a 2D hydrogen-bonding network that points into the solution and finally resulted in a LB-typed structure. The LB structure continues to grow into the laminated structure composed of alternative π-stacked layers and hydrogen-bonded layers. This crystal growth process lasted for ~20 s before the solvent was finally evaporated and the PYPA laminate crystals were deposited onto the substrate. This results in a polycrystalline stacked film. The green emission in the final stage becomes very weak due to the substantial quenching of fluorescence in solid state. Furthermore, a series of molecules including PYPDEt, ODPA, and PhPA were chosen on the basis of their capability for the formation of $\pi-\pi$ stacking and hydrogen bonding to testify this self-assembled mechanism and provide direct comparison to the PYPA molecule. The failure to achieve polycrystalline films from those molecules suggested that only the molecule forming both strong $\pi-\pi$ stacking and hydrogen bonding will allow the nucleation and growth of lamellar structure at the air/alcohol interface (see Supporting Information Figure S4).

To prove that the air/ethanol interface is the important media for the nucleation and growth of PYPA laminate crystals, a control experiment was performed by spin-coating PYPA solution in a closed chamber, which was saturated with ethanol vapor while all of the other experimental parameters were kept the same. The resulting morphology is shown in Figure 8, in which only small clusters of PYPA were formed on the surface without any crystalline laminate structure. This finding further supports the importance of the air/solvent interface in the self-assembly process.

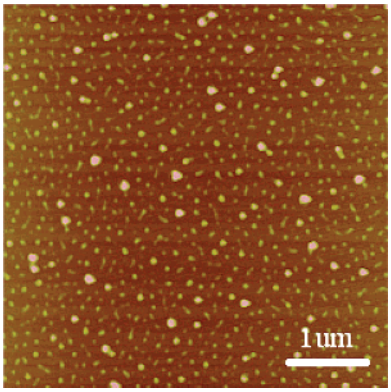

Figure 8. AFM image of PYPA aggregates spin-coated on SiO_2/Si substrate from 1 mM ethanol. The spin-coating process was performed under an enclosed system with saturated ethanol vapor.

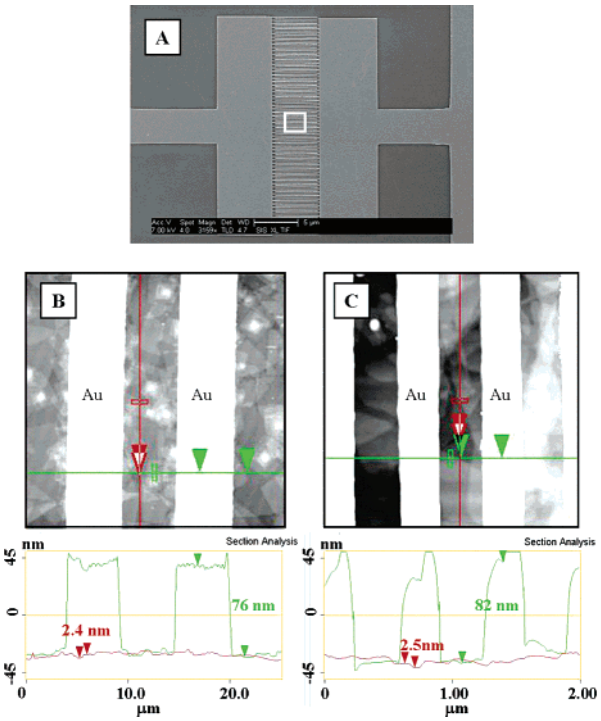

Figure 9. (A) SEM image of the inter-digitated Au finger electrodes on SiO_2/Si substrate. (B) and (C) are the height and cross-sectional images of PYPA polycrystalline films deposited on the Au fingers with 5 μm and 300 nm gap, respectively.

Deposition of Stacked Film on Structured Surface and Measurement of Its Electrical Properties. To explore the potential of using these polycrystalline PYPA stacked films for FETs, we have deposited the crystals on a structured SiO_2/Si substrate that was prepatterned with Au electrodes to test their electrical properties. The SEM image in Figure 9A shows the structure of the FET in which an array of inter-digitated Au electrodes with channel width varying from hundreds of nanometers to micrometers in size were deposited on a SiO_2-(60 nm)/n-Si substrate using e-beam lithography. The PYPA stacked films were deposited onto the patterned substrates by spin-coating from ethanol solution. The AFM height images in Figure 9B and C clearly show that the formation of the stacked PYPA film was not affected by the surface structure and the laminate crystals can fill and connect the gaps between the Au electrodes in both devices with 5 μm (Figure 9B) and 300 nm

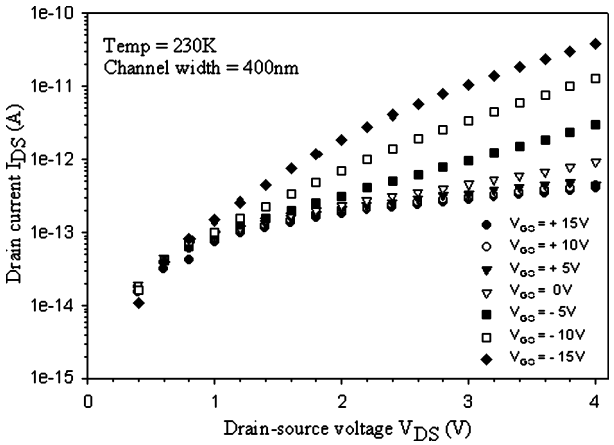

Figure 10. Plot of a drain current I_{DS} versus drain voltage V_{DS} at various gate voltages V_G from a bottom-contact OFET comprising the PYPA polycrystalline stacked film at 230 K. The gap width between the electrodes is 400 nm.

(Figure 9C) gaps. We assert the ability to transfer the crystalline PYPA stacked film to a patterned substrate without breaking the crystal structure based on several phenomena we observed earlier, including: (1) the stacked films can be deposited on an inert Au surface and a hydrophilic SiO_2/Si surface without destroying their crystalline structures; (2) the PYPA laminate crystal possesses a vertical slide plane so if the crystal partially lands on an Au finger, part of the crystal can still slide all of the way down to the SiO_2/Si substrate and make good contact with the Au electrode; and (3) the nucleation and growth of the self-assembled structure at the air/solvent interface allows the crystals to preorganize before they are physically deposited on the substrate surface. This solution processing approach provides not only a simple and inexpensive way to prepare crystalline π-conjugated films on patterned substrates but also circumvents the problem of inhomogeneous film formation at the edge of the metal electrode. The inhomogeneous region often contains a higher degree of morphological defeats, which is the main limiting factor in achieving high performance in bottom-contact FETs.[22]

To investigate the electrical property of the PYPA polycrystalline film that was deposited on the substrate with inter-digitated electrodes, we have carried out a series of measurements on devices with an electrode gap width of 400 nm. We have observed the modulation of drain current (I_{DS}) by a gate voltage (V_{GS}) at low temperatures. For example, the gating effect of the PYPA film was investigated at 230 K by measuring the I_{DS} versus V_{DS} at different gate voltages, and the results are shown in Figure 10. The strong dependence of mobility on the gate voltage at low temperature indicates the presence of traps in the PYPA stacked film. From the plot, we have confirmed that the PYPA film acts as a p-type semiconductor with a maximum on/off ratio of 1000 (defined as the ratio of current at $V_{GS} = -15$ V to current at $V_{GS} = 15$ V). Further study of the detailed charge transporting mechanism and performance of the PYPA stacked film will be published elsewhere.[23]

(22) Dimitrakopoulos, C. D.; Malenfant, P. R. L. *Adv. Mater.* **2002**, *14*, 99−117.
(23) Dong, J.; Yip, H. L.; Ma, H.; Jen, A. K. Y.; Parviz, B. A., submitted.

Conclusion

We have developed a simple and effective method to generate ordered 2D supramolecular structures through the interplay of strong H-bonding and $\pi-\pi$ stacking forces among 1-pyrylphosphonic acids. The formation of the crystalline laminate structure involves both nucleation and growth of crystals at the air/solvent interface. This self-assembly process is different from those reported for supramolecular structures that are formed in solution. Using this simple spin-coating process, we can deposit a polycrystalline PYPA stacked film on the SiO_2/Si substrate. The successful transfer of the stacked film onto a SiO_2/Si substrate prepatterned with Au electrodes has also been demonstrated. A gating effect on the charge transport of the polycrystalline films indicates that PYPA laminate crystal possesses p-typed semiconductor characteristics. Further improvements of the electrical properties of the supramolecular structures can potentially be achieved by applying this method to other aromatic phosphonic acids.

Acknowledgment. This work was supported by the Air Force Office of Scientific Research (AFOSR) under the Bio-inspired Concept Program and NSF Science and Technology Center for Materials and Devices for Information Technology Research (NSF DMR-0120967). A.K.-Y.J. thanks the Boeing-Johnson Foundation for financial support. H.-L.Y. and J.D. thank the Nanotechnology Fellowship sponsored by the University Initiative Fund (UIF) at the University of Washington for partially supporting this research.

Supporting Information Available: Materials synthesis, FTIR data of PYPA polycrystalline film, STM images of PYPA crystal on gold substrate, UV−vis absorption spectrum of PYPA films, AFM images and molecular structure of PYPDEt, ODPA, and PhPA, AFM height and phase images of PYPA polycrystalline film deposited on Au patterned SiO_2/Si substrate, and complete ref 7b. This material is available free of charge via the Internet at http://pubs.acs.org.

JA0563152